ELSEVIER

Ultrasound in Med. & Biol., Vol. ■, No. ■, pp. 1–10, 2015

0301-5629/$ - see front matter

http://dx.doi.org/10.1016/j.ultrasmedbio.2015.07.026

● *Original Contribution*

胎儿活动监测的多维超声多普勒信号分析

MULTIDIMENSIONAL ULTRASOUND DOPPLER SIGNAL ANALYSIS FOR FETAL ACTIVITY MONITORING

Sophie Ribes,* Jean-Marc Girault,† Franck Perrotin,‡ and Denis Kouamé*

*University of Toulouse III, IRIT UMR CNRS 5505, Toulouse, France; †University of Tours, INSERM U930 Tours, France; and ‡CHU Bretonneau, Tours, service de Gynecologie Obstétrique, INSERM U930, Tours, France

(*Received* 29 *July* 2014; *revised* 22 *July* 2015; *in final form* 27 *July* 2015)

胎儿活动参数(如运动、心率和相关参数)是胎儿健康的重要指标，没有任何设备能够同时获取和充分估计所有这些参数，以评估胎儿健康。这项工作的目的是收集这些参数，以自动分离健康的胎儿和受损的胎儿。为了实现这一目标，我们开发了多传感器多门多普勒系统。记录多维多普勒信号，并通过专用的信号处理技术估计胎儿活动参数。最后，我们将这些参数组合成四组参数(或四组超参数)，以确定能够将健康胎儿与其他胎儿分开的参数集。为了验证我们的系统，由医生建立并提供由两组信号(正常和受损)组成的数据集。根据估计的参数，计算出瞬时曼宁样评分，即超声评分，并将其与运动、心率及相关参数一起用于支持向量机方法的分类过程。我们研究了参数集的影响，并通过敏感性、特异性、支持向量百分比和总分类误差的计算来评估支持向量机的性能。四组的灵敏度范围为79%～100%。所有组的特异性均为100%。总的分类误差在0%～20%之间。支持向量的百分比在33%～49%之间。总的来说，采用胎儿运动、短期变异性、长期变异性、减速和超声评分等参数组的结果最好。该集合的灵敏度、特异度、支持向量百分比和总分类误差分别为100%、100%、35%和0%。这表明我们有能力将数据分为两组(正常胎儿和病理胎儿)，结果突出了与医生进行的临床分类的极佳匹配。这项工作表明了检测受损胎儿的可行性，也代表了一个有趣的方法，密切监测胎儿在整个怀孕期间。

Abstract—Fetal activity parameters such as movements, heart rate and the related parameters are essential indicators of fetal wellbeing, and no device provides simultaneous access to and sufficient estimation of all of these parameters to evaluate fetal health. This work was aimed at collecting these parameters to automatically separate healthy from compromised fetuses. To achieve this goal, we first developed a multi-sensor–multi-gate Doppler system. Then we recorded multidimensional Doppler signals and estimated the fetal activity parameters via dedicated signal processing techniques. Finally, we combined these parameters into four sets of parameters (or four hyperparameters) to determine the set of parameters that is able to separate healthy from other fetuses. To validate our system, a data set consisting of two groups of fetal signals (normal and compromised) was established and provided by physicians. From the estimated parameters, an instantaneous Manning-like score, referred to as the ultrasonic score, was calculated and was used together with movements, heart rate and the associated parameters in a classification process employing the support vector machine method. We investigated the influence of the sets of parameters and evaluated the performance of the support vector machine using the computation of sensibility, specificity, percentage of support vectors and total classification error. The sensitivity of the four sets ranged from 79% to 100%. Specificity was 100% for all sets. The total classification error ranged from 0% to 20%. The percentage of support vectors ranged from 33% to 49%. Overall, the best results were obtained with the set of parameters consisting of fetal movement, short-term variability, long-term variability, deceleration and ultrasound score. The sensitivity, specificity, percentage of support vectors and total classification error of this set were respectively 100%, 100%, 35% and 0%. This indicated our ability to separate the data into two sets (normal fetuses and pathologic fetuses), and the results highlight the excellent match with the clinical classification performed by the physicians. This work indicates the feasibility of detecting compromised fetuses and also represents an interesting method of close fetal monitoring during the entire pregnancy. (E-mail: kouame@irit.fr) © **2015 World Federation for Ultrasound in Medicine & Biology.**

Key Words: **Fetal monitoring, Fetal heart rhythm, Fetal movement, Multidimensional signals, Support vector machine.**

胎儿监护，胎儿心律，胎儿运动，多维信号，支持向量机。

INTRODUCTION

Fetal monitoring may be required at different times during pregnancy to closely monitor certain fetal and maternal disorders (Manning et al. 1980). Existing methods, which consist of asking women to count the number of fetal movements, performing a biophysical profile or Manning's test (Manning et al. 1980) or analyzing general movements, may be either subjective or time consuming. To automatically monitor fetal activity, the most commonly used system is the cardiotocogram. This device measures fetal heart rate (FHR) and uterine contractions (Royal College of Obstetricians and Gynecologists [RCOG] 2001) but does not provide any information regarding fetal movements. This may explain why the performances of major classifiers, which are based on FHR variability analysis alone (through different kind of entropies), are on the order of 80% for specificity and 80% for sensitivity (Ferrario et al. 2006). We believe that additional information may improve classification performance. There are many dedicated ultrasound systems that collect additional information such as fetal movement and pseudo-breathing. Unfortunately, these systems provide only partially automated detection of fetal movement (Karlsonn et al. 2000a) or breathing (Karlsonn et al. 2000b; Yamakoshi et al. 1996).

Address correspondence to: Denis Kouamé, 118 rte de Narbonne, F31062 Toulouse, France. E-mail: kouame@irit.fr

妊娠期间可能需要在不同时间进行胎儿监测，以密切监测胎儿和产妇的某些疾病(Manning etal . 1980)。现有的方法包括要求妇女数胎儿运动的次数，进行生物物理分析或曼宁测试(Manning etal . 1980)，或分析一般的运动，可能是主观的或耗时的。为了自动监测胎儿活动，最常用的系统是心率描记仪。该设备测量胎儿心率(FHR)和子宫收缩，但不提供任何有关胎儿运动的信息。这可能解释了为什么主要分类器的性能仅基于FHR变异性分析(通过不同类型的熵)，在特异性和敏感性方面分别是80%和80%，我们相信额外的信息可以提高分类性能。有许多专门的超声系统收集额外的信息，如胎儿运动和假呼吸。不幸的是，这些系统只能部分自动检测胎儿运动或呼吸

Some preliminary attempts to overcome these limitations were made by Kribèche et al. (2007). The main characteristic of their system is that, because of the large number of sensors needed to cover an explored area as large as possible, a large number of Doppler signals have to be processed. The aim of our work was not to develop new signal processing methods and evaluate their performance. Instead, we sought to efficiently combine some relevant existing signal processing techniques to achieve the following goals: extract fetal activity features, such as FHR and movements (and related features), and efficiently collect these features to differentiate between normal and potentially compromised fetuses. To achieve these goals, we needed first to reduce the inherent redundancy related to the large number of acquired Doppler signals and then to separate fetal from maternal signals through a blind source separation. The detailed signal processing algorithms used to extract the fetal activity parameters are not detailed here. The reader is referred to, for example, Rouvre et al. (2005), Voicu (2011) and Voicu et al. (2010, 2014). However, even if the number of relevant data can be reduced, a fusion step is required to provide the physical with global information, for example, an "ultrasound score," on which a decision can be based.

我们工作的目的不是开发新的信号处理方法并评估它们的性能。相反，我们寻求有效地结合一些相关的现有信号处理技术，以实现以下目标:提取胎儿活动特征，如FHR和运动(及相关特征)，并有效地收集这些特征来区分正常和潜在的受损胎儿。为了实现这些目标，我们首先需要减少与大量获取的多普勒信号相关的固有冗余，然后通过盲源分离将胎儿与母体信号分离。

然而，即使可以减少相关数据的数量，也需要一个融合步骤来为物理提供全面的信息，例如，一个"超声评分"，可以作为一个决定的基础。

Thus, the main challenge of this study, and its incremental value with respect to the previously published article (Kribèche et al. 2007), was to develop a method that enables extraction of the relevant information necessary to construct a global indicator sufficiently pertinent to classify fetuses into normal and potentially compromised groups. To validate the feasibility, this method was successfully tested on a heterogeneous data set obtained from pregnant women and composed of FHR, movement and pseudo-breathing signals. To our knowledge, this automated classification is a new and important contribution to the search for an objective method for monitoring fetal activity, which remains an open issue (Grivell et al. 2010; Kaluzynskia et al. 2011).

因此，本研究的主要目的是开发一种方法，能够提取必要的相关信息，从而构建一个足够相关的全局指标，将胎儿分类为正常和潜在的受损群体。为验证该方法的可行性，在孕妇的FHR、运动和伪呼吸信号组成的异构数据集上进行了成功的测试。

This article is arranged as follows: We first described the device produced by an industrial collaboration and used for this study, and then briefly introduce the signal processing techniques used. The ultrasound score is then introduced and investigated using fetal activity parameters obtained from real fetal Doppler signals. Finally, results from classification of sets of fetuses are discussed.

本文的安排如下:我们首先描述了一个工业协作生产的用于本研究的设备，然后简要介绍了所使用的信号处理技术。然后引入超声评分，并使用从真实胎儿多普勒信号获得的胎儿活动参数进行调查。最后，讨论了胎儿组分类的结果。

MATERIALS AND METHODS

Materials

We constructed, in collaboration with Althais Technologies (Tours, France), a multi-sensor Doppler system (Surfoetus) that was able to monitor most parts of the fetal body. Although a complete description of the development of this device is beyond the scope of this article, we briefly provide here a brief description. The system consists of 12 ultrasound (US) sensors, each with five gates, working at a frequency of $f_0 = 2$ MHz and an electronic US device (three electronic pulsed Doppler boards and one data acquisition board). A low-noise amplifier amplifies the received signal; a deep compensated amplifier then balances the strong attenuation of the deepest gates. After complex demodulation and filtering, the Doppler components are sampled sequentially and converted. Sampling frequency, denoted F_e, is 1 kHz. Five adjustable gates ranging from 2 to 14 cm are used to explore the depths. These 12 sensors are divided into three groups of four sensors, as illustrated in Figure 1. Group A (US sensors 1–4) is used to explore the fetal thorax, investigating FHR and breathing movements; group B (sensors 5–8) the upper limbs; and group C (sensors 9–12) the lower limbs. Each sensor is a circular piezoelectric element 12 mm in diameter. The ultrasound beam was not focused. A belt was used during recording to maintain all three groups.

我们与althai Technologies (Tours, France)合作构建了一个多传感器多普勒系统(Surfoetus)，能够监测胎儿身体的大部分部位。虽然对这种设备的开发的完整描述超出了本文的范围，但我们在这里简要地提供一个简要描述。该系统由12个超声波(US)传感器组成，每个传感器有5个门，工作频率为f0 5 2 MHz和一个电子US设备(三个电子脉冲多普勒板和一个数据采集板)。低噪声放大器放大接收信号;然后用深补偿放大器来平衡最深门的强衰减。经过复杂的解调和滤波后，对多普勒分量进行采样和转换。采样频率为1 kHz，记为Fe。5个可调节的门，范围从2到14厘米，用于探索深度。这12个传感器被分为3组，每组4个传感器，如图1所示。A组(US传感器1-4)探查胎儿胸腔，观察FHR及呼吸运动;B组(传感器5～8个)上肢;C组(传感器9-12)用于下肢。每个传感器是一个直径12毫米的圆形压电元件。超声波光束没有聚焦。录音过程中使用了皮带来保持所有三个组。

协议 *Protocol*

介绍了参与研究的孕妇，及符合研究标准的孕妇条件实验安排和实验数据

In this study, 44 pregnant women at a gestational age >24 weeks were prospectively enrolled. Inclusion criteria were singleton pregnancy, absence of significant maternal complications requiring premature delivery (hypertensive disorders; renal, heart or immunologic pathology; pre-existing diabetes), willingness to have pregnancy followed or delivered locally, maternal age >18 years and health insurance affiliation. Exclusion criteria were fetal malformation, maternal significant complications, pregnancy care in another center and concomitant participation in another research protocol. This study was approved by the University's ethics committee (Clinical Investigation Centre, Innovation

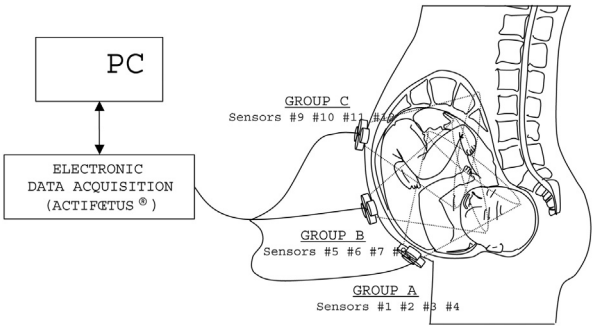

Fig. 1. Sensor group arrangement. Group A (sensors 1–4) explores the fetal thorax, investigating fetal heart rate and breathing movements. Group B (sensors 5–8) explores the upper limbs, and group C (sensors 9–12), the lower limbs. A belt is used during recording to prevent sensor movement.

图1所示。传感器组安排。A组(传感器1-4)探查胎儿胸腔，调查胎儿心率和呼吸运动。B组(传感器5-8)探测上肢，C组(传感器9-12)探测下肢。记录时使用皮带，防止传感器移动

Technology, Ethics). The ethics ID number was 2004-32, and the study number was CT04-SURFOETUS. All participants submitted a signed informed consent.

The standard demographic measures, expressed as the mean ± standard deviation (range) were age = 29.9 ± 5.9 (20–44) years, height = 164 ± 6 (151–179) cm and weight = 63.23 ± 15.88 (41–123) kg. Pregnancies were classified in two groups: normal and IUGR (intrauterine growth restriction) depending on ultrasound-estimated fetal growth at inclusion. IUGR was defined as an estimated fetal weight under the 10th percentile or a transverse abdominal perimeter below the 10th percentile for gestational age. All recordings were performed between the 24th and 40th weeks of gestation in the Obstetrics Department of Bretonneau University Hospital, Tours, France. In the "normal" group, recordings were performed every 4 weeks, and in the "IUGR" group, recordings were performed every 2 weeks. The overall mean gestational age was 30.2 weeks (median = 32 weeks). The mean gestational age of the normal group was 30.1 weeks, and the mean gestational age of the IUGR group was 29.9 weeks.

Overall, we obtained 98 Doppler signals for the 44 patients. Each examination in this protocol was 30 min long. The first group, referred to as "normal pregnancies," consisted of 74 measurements and 31 subjects. The second group, referred to as "pathologic pregnancies" or "group with IUGR" consisted of 24 measurements and 13 subjects.

Procedures

As mentioned earlier, the electronic control system is composed of 12 sensors with five gates per sensor, and thus, 60 complex Doppler signals must be processed each millisecond. This is a very large amount of data with inevitable redundancy in the signals. Furthermore, as the signals recorded from different sensors originate from different sources of signals (fetal heart movement, maternal heart movement, respiration, *etc.*), a source separation is strongly expected to extract fetal signal only. Assuming that there is an L-dimensional zero-mean signal source vector $s(t) = [s_1(t), \ldots, s_L(t)]^T$, and an M-dimensional data vector $x(t) = [x_1(t), \ldots, x_M(t)]^T$ observed at each time point t. In short, L is the number of sources, and M is the number of observable mixed data. L and M are generally different. These signals can be modeled as

$$x(t) = A.s(t) + u(t) \quad (1)$$

where x represents the signals observed or acquired by the sensors, referred to below as the "observation matrix"; A is the mixing matrix, corresponding to maternal body "mixing"; s is the unobservable source matrix; and $u(t)$ is a zero-mean Gaussian noise vector with a covariance matrix Λ. In summary, we have different source signals denoted s non-observable, which are mixed and acquired by the sensors and denoted x. As stated before, the fetal signals need to be extracted and separated to correctly monitor fetal activity. To perform an unsupervised source separation, that is, without any *a priori* information, the number of independent sources must be evaluated from our data set. To do so in a parsimonious way, a redundancy information reduction must be performed.

Dimension reduction and sparse blind source separation

From the set of data, we perform dimension reduction to eliminate the data redundancy (see Appendix A). We searched for the number of independent sources using the method described in Appendix A. This number of independent sources was found to be two or three. Knowing the number of sources, we performed signal separation to separate the fetal Doppler signal from the mother's signal (see Appendix B). The last technique to be explored concerned the statement of a meta-descriptor allowing an objective evaluation of fetal state.

Ultrasound score

To compute an objective parameter including information on fetal heart rate and fetal movements, we introduced a Manning-like hyper-parameter referred to as the ultrasound score (Ribes et al. 2011). This meta-descriptor was computed every minute during each examination, as explained later. The ultrasound score is the sum of five values denoted $V1$, $V2$, $V3$, $V4$ and $V5$ that are based on the estimated fetal activity parameters, as reported in Table 1.

$V1$ and $V2$ were both based on the fetal heart rate, which is an essential component in the follow-up of pregnancies (Rouvre et al. 2005; Voicu et al. 2010) because it is correlated with fetal health. As reported in Table 1, $V1$ represents the baseline (or mean value of FHR), and $V2$ represents the variance of the baseline. This baseline is the mean FHR computed when the variability was between 5 and 25 bpm over 1 minute. The baseline is rounded to increments of 5 bpm during a 10-min segment. The normal value lies between 110 and 160 bpm. Detection of the FHR may be improved using a specific prior (Manning 1977).

Table 1. Ultrasound score: Parameters computed each minute, associated variables and resulting points

Parameter	Variable	Points
Baseline	$V1$	1.5 to 2
Baseline variance	$V2$	−1.5 to 1
Upper limb movements	$V3$	0 to 1
Lower limb movements	$V4$	0 to 1
Offset	$V5$	2

$V3$ and $V4$ are both based on limb movements. $V3$ represents upper limb movements whereas $V4$ represents lower limb movements. These movements can be detected either on the separated magnitudes by their sudden changes or by searching for the increase or decrease in the overall phase. However, to eliminate false detection caused by phase noise, detection of fetal movement was combined with a threshold algorithm (Karlsonn et al. 2000b). In this algorithm a movement was defined by a magnitude level above the noise threshold with a minimum duration of 0.2 s, followed by a minimum rest duration of 0.5 s.

Finally, $V5$ is an offset.

The empirical range of values was chosen on the following basis:

- If the baseline was >110 or <160 bpm, the value of $V1$ was set between 1.5 and 2; otherwise $V1$ was set at 0. More precisely, let BL denote the baseline. Thus, $V1$ is defined as $V1 = 0.01(BL-110)+1.5$ if $110 \leq BL \leq 160$, $V1 = 0$ otherwise.
- If the baseline variance was <17.5, then the value of $V2$ was set between 0 and 1; if the baseline variance was >17.5, but <22.5, then the value of $V2$ was set between -1.5 and 1; otherwise, the value of $V2$ was set at -1.5. More precisely, let BLV denote the baseline variance (which is a positive value). Thus $V2$ is defined by $V2 = BLV/17.5$ if $0 \leq BLV \leq 17.5$; $V2 = -0.5(BLV-17.5)+1$ if $17.5 < BLV \leq 22.5$; and $V2 = -1.5$ if $BLV > 22.5$.
- If two or more upper limb movements were detected, the value of $V3$ was set at 1; otherwise $V3$ was set at 0. If two or more lower limb movements were detected, then the value of $V4$ was set at 1; otherwise the value of $V4$ was set to 0.
- To have a positive ultrasound score, we added an offset through V5 which is set at 2.

The ultrasound score for the complete recording was the mean of the ultrasound score computed for each minute. Figure 2 illustrates an example of the ultrasound score. At the top are the mean FHR and the standard deviation for each minute. In the middle are the numbers of movements detected from the upper limbs (*blue*) and lower limbs (*magenta*). At the bottom is the ultrasound score calculated from the aforementioned parameters.

As the parameters do not have the same importance in the follow-up of fetal well-being, we investigated different sets of parameters through four new parameters referred to as hyper-parameters:

- Hyper-parameter 1 consisted of baseline, fetal movement and ultrasound score.
- Hyper-parameter 2 consisted of baseline, fetal movement, short-term variability and ultrasound score.
- Hyper-parameter 3 consisted of baseline, fetal movement and short-term variability.
- Hyper-parameter 4 consisted of fetal movement, short-term variability, long-term variability, deceleration and ultrasound score.

Note that variability is the fluctuation in the FHR, quantified as the amplitude peak-to-peak trough in beats per minute. Short-term variability (STV) of FHR is commonly used in prediction of fetal distress. STV is the oscillation of the FHR around the baseline in amplitudes of 5 to 25 bpm, measured on time windows of 3.75 s. Long-term variability is the mean value over a minute (*i.e.*, the difference between the highest and the lowest values of FHR).

Recall of used support vector machine method

To find the best hyper-parameter, we propose the use of support vector machine (SVM) classification. Different classification methods were evaluated (Duda et al. 2001), and the SVM method (Ferrario et al. 1999; Vapnik 1995) was better able to classify the current data. To ensure a better understanding, the principles of SVM classification are provided in Appendix C. In this study and using SVM principles, a score optimization problem can be reformulated as a classification problem. The problem under consideration was the study of the separability of the data (normal fetuses vs. compromised fetuses), using only estimation of the hyper-parameters mentioned earlier. We had a classification problem in which the kernel function, the set of hyper-parameters, the kernel function features and the value of the constraint C had to be chosen. The choice of kernel functions was studied empirically, and optimal results were achieved using a polynomial kernel function defined by

$$K(\mathrm{x}, \mathrm{x}') = (1+x.x\prime)^d \qquad (2)$$

where d is the degree defined by the user. To obtain the best results, the SVM was computed using a polynomial kernel function for different sets of hyper-parameters, kernel degrees and a constraint C defined by the user.

First, the data was pre-processed to separate the signals of the mothers from those of the fetuses, and then the parameters listed in Table 1 were computed. The effectiveness of the SVM classification was evaluated using the computation of specificity, sensitivity, percentage of support vectors and total classification accuracy defined as follows:

- Specificity is the number of true-negative decisions divided by the number of normal pregnancies.
- Sensitivity is the number of true-positive decisions divided by the number of abnormal pregnancies.

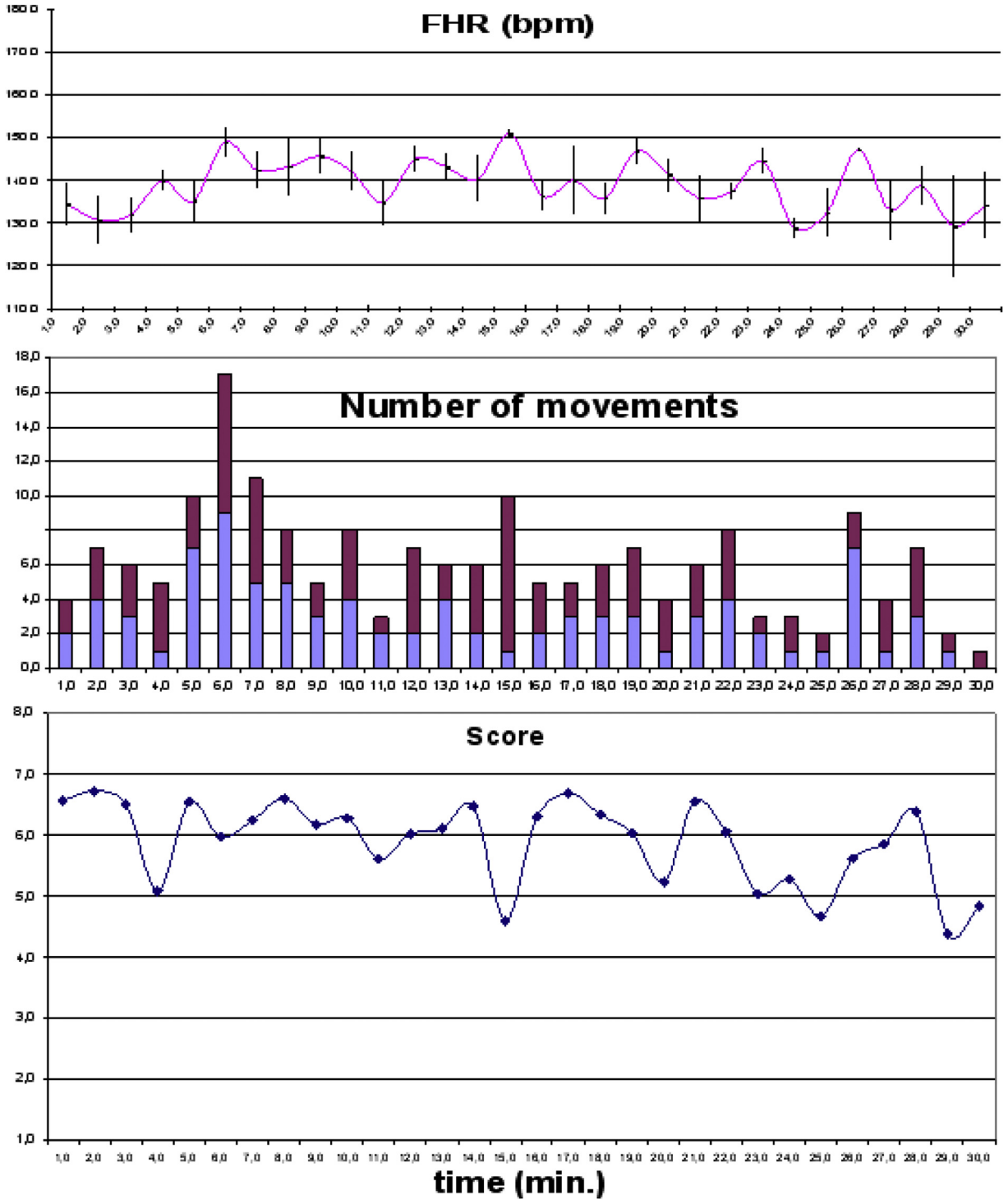

Fig. 2. Top: Mean fetal heart rate and mean STV each minute. Middle: Number of movements of the upper limbs (*blue*) and lower limbs (*purple*). Bottom: Ultrasound score calculated according to parameters. FHR = fetal heart rate; STV = short-term variability.

- Percentage of support vectors is the number of support vectors divided by the number of pregnancies.
- Classification accuracy is the number of correct decisions divided by the number of pregnancies.

A true-negative decision occurred when the classifier and the physician suggested the absence of positive detection. A true-positive decision occurred when the classifier and the physician suggested a positive

detection. As mentioned previously, a binary clinical classification (normal pregnancies and pregnancies associated with IUGR disorders) was performed by physicians.

RESULTS

We first searched for the best hyper-parameter. For different kernel degrees d and different constraints C, we performed the classification process and compared classification accuracies. Figure 3 illustrates the relationship between total error and constraint for the different hyper-parameters: for all hyper-parameters, total error decreased when constraint C increased. Hyper-parameters 2 and 3 differed only by consideration of the ultrasound score, and hyper-parameter 2, which contained this parameter, always yielded greater accuracy than hyper-parameter 3, confirming that inclusion of the ultrasound score facilitated and improved the classification process. For all constraint C values, hyper-parameter 4 always yielded the best results, and we chose to investigate only this hyper-parameter in the remainder of our study.

To find the optimal degree of the polynomial kernel function, we evaluated the performance of the classification considering hyper-parameter 4 and increasing constraint C for different degrees, as illustrated in Figure 4. Higher degrees offered more general solutions, with a reduction in the number of support vectors, projecting data into a higher-dimensional space and providing a lower error rate. At the same time, if we chose to use high levels of constraint C, we obtained better classification accuracy. The trade-off between the complexity of the decision region and the training error rate can be monitored by changing parameter C.

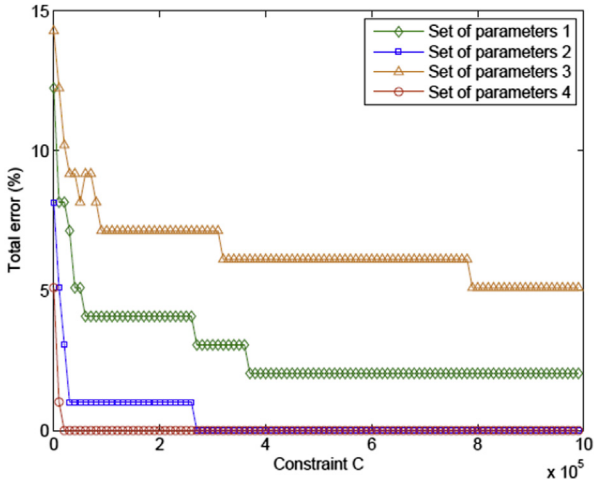

Fig. 3. Comparison of the total error for all hyper-parameters and various constraints for a degree value $d = 15$. Hyper-parameter 4 was always better.

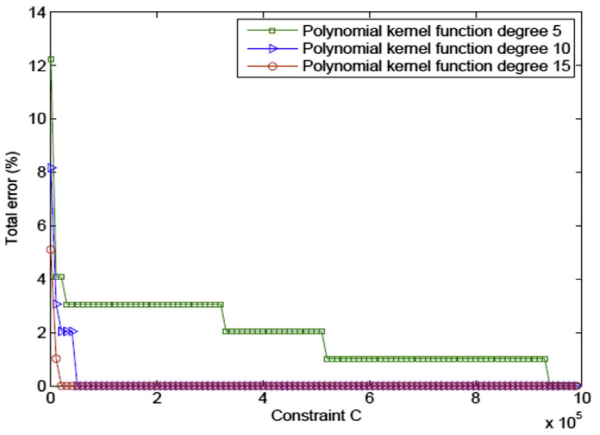

Fig. 4. For various values of constraints and various degrees of kernel, the total error made for hyper-parameter 4 is evaluated. High degrees and high constraints provided better results.

Once the effects of the degree, constraint and set of hyper-parameters had been studied, the results summarized in Tables 2 and 3 were obtained for a degree value $d = 15$ and a constraint value $C = 9.0 \times 10^5$ for all sets of hyper-parameters. Table 2 outlines the distribution of normal pregnancies, and Table 3, the distribution of pregnancies that presented with IUGR disorders. Zones 1–4, revealed by the classifier, corresponded to areas related to the hyper-planes found, as illustrated in Figure 5. Zones 1 and 4 are the areas in which the fetuses were classified without any doubt as normal and compromised, respectively. Zones 2 and 3 provided trends and were associated with probable normality for zone 2 and probable compromise for zone 3. It can be seen in Table 2, for all sets of hyper-parameters, that the normal pregnancies were found only in zones 1 and 2, that is, in the zones of normality. In Table 3, for the sets of hyper-parameters 2 and 4, it can be seen that no pregnancy was classified in zones 1 and 2; there were no false-negative decisions. From these two tables, we can

Table 2. Distribution of normal pregnancies, polynomial kernel function, degree $d = 15$, constraint $C = 9.0 \times 10^5$*

	Hyper-parameter			
Zone	1	2	3	4
1	75.67%	68.91%	64.86%	68.91%
2	24.32%	31.08%	35.13%	31.08%
3	0	0	0	0
4	0	0	0	0

* Zones 1–4 were provided by the classifier and corresponded to a location related to the three hyperplanes. Zones 1 and 4 were the zones where the fetuses were clearly classified as normal fetuses and as fetuses presenting intrauterine growth retardation disorders, respectively. Zones 2 and 3 provided trends and were associated with probable normality for zone 2 and probable disorder for zone 3.

Table 3. Distribution of the pregnancies presenting with disorders, polynomial kernel function, degree $d = 15$, constraint $C = 9.0 \times 10^5$*

	Hyper-parameter			
Zone	1	2	3	4
1	4.16%	0	8.33%	0
2	4.16%	0	12.5%	0
3	50%	58.33%	70.83%	50
4	41.66%	41.66%	8.33%	50

* Zones 1–4 were provided by the classifier and corresponded to location related to the three hyperplanes. Zones 1 and 4 were the zones where the fetuses were clearly classified as normal fetuses and as fetuses presenting with intrauterine growth retardation disorders, respectively. Zones 2 and 3 provided trends and were associated with probable normality for zone 2 and probable pathology for zone 3.

conclude that hyper-parameters 1–4 can identify all normal pregnancies (Table 2), and hyper-parameters 2 and 4 can identify all pregnancies that present with an IUGR disorder (Table 3).

It should be noted that we were able to identify all normal pregnancies (Table 2) and all pathologic pregnancies (Table 3), and these were good results concerning the separability of the data. Table 4 provides the overall results using evaluation of sensitivity and specificity. It can be seen that all sets of hyper-parameters, including the ultrasound score, yielded better results. Sensitivity, specificity and total error rate were excellent for hyper-parameters 2 and 4, which confirms the separability of the data in a high-dimensional space. According to the percentage of support vectors, we suggest use of hyper-parameter 4, which used fewer support vectors during the learning stage. Note also that the specificity and sensitivity values included the support vector.

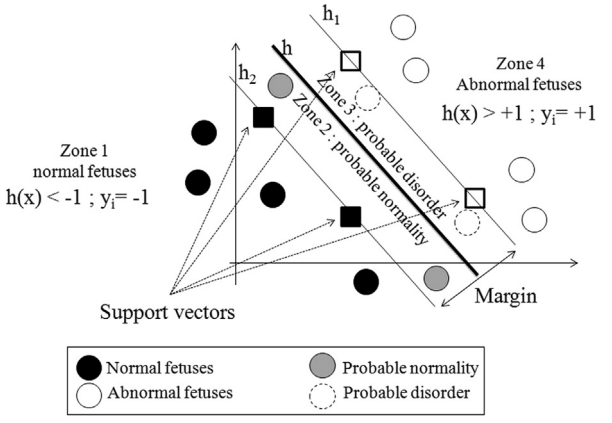

Fig. 5. Support vector machine classification. Zones 1–4 are provided by the classifier and correspond to areas related to the hyperplanes. Zones 1 and 4 are the areas where the fetuses were classified respectively as normal fetuses and as abnormal fetuses. Zones 2 and 3 provide respectively trends of probable normality and probable disorder.

Table 4. Overall evaluation: the total error, the percentage of support vectors, the sensitivity and the specificity were computed for all hyper-parameters

	Hyper-parameter			
	1	2	3	4
Total error	20.4%	0	5.1%	0
Support vectors	32.65%	37.75%	48.97%	35.71%
Sensitivity	91.66%	100%	79.16%	100%
Specificity	100%	100%	100%	100%

DISCUSSION AND CONCLUSIONS

We have illustrated in this work that combining some efficient and dedicated signal processing techniques for extraction of fetal activity features (fetal heart rhythm, variabilities, fetal limb, accelerations) can enable close separation of normal from compromised fetuses. To do so we introduced an ultrasound score, including the parameters fetal heart rate value, short-term variability and numbers of movements of the upper and lower limbs. We combined this score and other fetal activity parameters to obtain different hyper-parameters. Using these hyper-parameters and a SVM classification method, we illustrated the ability of our system to separate data into two sets, normal pregnancies and pathologic pregnancies, and obtained excellent matches to clinical classifications performed by physicians. These are valuable results and indicate an interesting way forward for home fetal monitoring. To our knowledge, this system is unique.

This study had two main limitations that will be investigated in our future works: binary classification and limited validation. With respect to binary classification, we considered here two groups (normal and IUGR). Different types of pathologies and subgroups of pathologies, with different stages, could be valuable in testing the robustness of our method. As for limited validation, the study was performed in a single clinical center. Using data from different clinical centers and performing classification of new and independent data would also help to enhance the validity of the methods on a large scale.

我们已经在这项工作中说明，结合一些有效和专用的信号处理技术提取胎儿活动特征(胎儿心率、变异性、胎儿肢体、加速)，可以使正常和受损胎儿紧密分离。为此，我们引入了超声评分，包括胎儿心率值、短期变异性和上下肢运动次数等参数。我们将此评分与其他胎儿活动参数结合，得到不同的超参数。使用这些超参数和支持向量机分类方法，我们展示了我们的系统将数据分为正常妊娠和病理性妊娠两组的能力，并获得了与医生进行的临床分类的良好匹配。这些是有价值的结果，并指出了一个有趣的方式，以家庭胎儿监测。据我们所知，这个系统是独一无二的。本研究有两个主要的局限性，将在我们未来的工作中进行研究：二元分类和有限验证。对于二元分类，我们在这里考虑两组(正常和IUGR)。不同类型的病理和不同阶段的病理子组在测试我们方法的稳健性方面可能很有价值。在有限验证方面，本研究在单一临床中心进行。使用来自不同临床中心的数据，对新的独立数据进行分类，也有助于大规模提高方法的有效性。

Acknowledgments—This study was supported by the Agence Nationale de la Research (Project ANR-07-TECSAN-023, Surfoetus) and performed with CIC-IT 1415, Tours. We warmly thank Laurent Colin, Philippe Vince, Fabrice Gens and Thierry Pottier from Althias University of Tours, Tours, France; Catherine Roussel and Morgane Fournier-Massignan from CHU Bretonneau Tours, France; and Dr. Iulian Voicu.

REFERENCES

Attias H. Independent factor analysis. Neural Comput 1999;11: 803–851.

Bingham E, Hyvarinen A. A fast fixed-point algorithm for independent component analysis of complex valued signals. Int J Neural Syst 2000;10:1–8.

Cardoso JF. Blind signal separation: Statistical principles. Proc IEEE 1998;9:2009–2025.
Cardoso JF. Higher-order contrasts for independent component analysis. Neural Comput 1999;11:157–192.
Davis M, Mitinoudis N. A simple mixture for sparse overcomplete ICA. IEE Proc Vision Image Signal Process 2004;151:35–43.
Duda R, Hart P, Stork D. Pattern classification. 2nd ed. New York: Wiley; 2001.
Ferrario M, Signorini MG, Magenes G, Cerutti S. Support-vector networks. Mach Learn 1999;20:273–297.
Ferrario M, Signorini MG, Magenes G, Cerutti S. Comparison of entropy-based regularity estimators: Application to the fetal heart rate signal for the identification of fetal distress. IEEE Trans Biomed Eng 2006;53:119–125.
Grivell R, Alfirevic Z, Gyte G, Devane D. Antenatal cardiotocography for fetal assessment (review). Cochrane Database Syst Rev 2010; 1:CD007863.
Ikeda S, Toyama K. Independent component analysis for noisy data: MEG data analysis. Neural Netw 2000;13:1063–1074.
Kaluzynskia K, Kreta T, Czajkowskib K, Sienkob J, Zmigrodzkia J. System for objective assessment of fetal activity. Med Eng Phys 2011; 33:692–699.
Karlsonn B, Berson M, Helgason T, Geirsson R, Pourcelot L. Effect of fetal and maternal breathing on the ultrasonic Doppler signal due to fetal heart movement. Eur J Ultrasound 2000a;11:47–52.
Karlsonn B, Foulquière K, Kaluzynski K, Tranquart F, Fignon A, Pourcelot D, Pourcelot L, Berson M. The Dopfet system: A new ultrasonic Doppler system for monitoring and characterisation of fetal movement. Ultrasound Med Biol 2000b;26:1117–1124.
Kribèche A, Tranquartlow F, Kouame D, Pourcelot L. The Actifetus system: A multidoppler sensor system for monitoring fetal movements. Ultrasound Med Biol 2007;33:430–438.
Lee TW. Independent component analysis: Theory and applications. Norwell, MA: Kluwer Academic; 1998.
Mallat S. A wavelet tour of signal processing. Orlando, FL: Academic Press; 1998.
Manning F. Fetal breathing movement as a reflexion of fetal status. Postgrad Med 1977;61:116–122.
Manning F, Platt L, Sipos L. Antepartum fetal evaluation: Development of a fetal biophysical profile. Am J Obstet Genicol 1980;136:787–795.
Ribes S, Kouamé D, Voicu I, Fournier-Massignan M, Perrotin F, Tranquart F. Support vector machines based multidimensional signals classification for fetal activity characterization. SPIE Med Imaging 2011;7968:79680D.
Rouvre D, Kouamé D, Tranquart F, Pourcelot L. Empirical mode decomposition (EMD) for multi-gate, multi-transducer ultrasound Doppler fetal heart monitoring. In: Proceedings, Fifth IEEE International Symposium on Signal Processing and Information Technology. New York: IEEE; 2005. p. 208–212.
Royal College of Obstetricians and Gynaecologists (RCOG). The use of electronic fetal monitoring: The use and interpretation of cardiotocography in intrapartum fetal surveillance. London: RCOG Press; 2001.
Touretzky DS, Mozer MC, Hasselmo ME, (eds). Advances in neural information processing systems, Vol 8. Cambridge, MA: MIT Press; 1996. p. 145–151.
Vapnik V. The nature of statistical learning theory. Berlin/Heidelberg: Springer-Verlag; 1995.
Voicu I, Girault J, Fournier-Massignan M, Kouamé D. Robust estimation of fetal heart rate form US Doppler signals. Phys Proc 2010; 3:691–699.
Voicu I. Analysis, characterization and classification of fetal signals. PhD thesis; 2011 [In French].
Voicu I, Ménigot S, Kouamé D, Girault J. New estimators and guidelines for better use of fetal heart rate estimators with Doppler ultrasound devices. Comput Math Methods Med 2014;784862.
Yamakoshi Y, Shimizu T, Shinozuka N, Masuda H. Automated fetal breathing movement detection from internal small displacement measurement. Biomed Tech 1996;41:242–247.

APPENDIX A

DIMENSION REDUCTION

We investigated different methods of estimating the number of sources in an observation matrix such as the maximum description length, Bayesian information criterion and Akaike information criterion (AIC), which was the most suited to our data set (see also Ikeda and Toyama 2000). For convenience, model (1) can be rewritten in the framework of factor analysis as

$$x = Bf + \mu + \varepsilon \tag{A.1}$$

where f is normally distributed as $f \sim N(0, I_m)$ and I_m is the $m \times m$ identity matrix; ε is normally distributed as $\varepsilon \sim N(0, \Sigma)$; and Σ is a diagonal matrix $L \times L$. f and ε are mutually independent. Signals are analyzed in short stationary windows, and therefore, because of the stationarity of ε, μ and f, for convenience in eqn (A.1) we voluntarily ignore the time variable t. The mean of x is given by μ, which is assumed here to be zero. The optimum number of sources is then estimated using the AIC.

$$\left(\widehat{B}, \widehat{\Sigma}\right)_{MLE} = \operatorname{argmax}\Big|_{B,\Sigma} L(B, \Sigma) \tag{A.2}$$

where C_x is the covariance matrix of x and

$$L(B, \Sigma) = -\frac{1}{2}\left\{\operatorname{tr}\left(C_x(\Sigma + BB^T)^{-1}\right) + \log(\det(\Sigma + BB^T)) + L\log(2\pi)\right\}$$

For a set of data $\mathrm{x}(t = 1, \cdots, N)$, the AIC is then defined as

$$AIC = -L\left(\widehat{B}, \widehat{\Sigma}\right) + \frac{2}{N}\left(L(m+1) - \frac{m(m-1)}{2}\right) \tag{A.3}$$

where

$$m \leq Q = \frac{1}{2}\left\{2L + 1 - \sqrt{8L+1}\right\} \tag{A.4}$$

To estimate the number of sources in the mixture x, we first estimated B and Σ for $1 \leq m \leq Q$, m being defined by eqn (A.4). The correct number of sources m was the one that minimized the AIC. The correct number of sources is important *a priori* information to perform source separation which gives the dimensions of the mixing matrix A to be evaluated.

Once the redundancy was reduced, the next important step was to separate the different sources in an unsupervised manner.

APPENDIX B

SPARSE BLIND SOURCE SEPARATION

Independent component analysis (ICA) is one of the best known techniques used for blind source separation. It aims at recovering unobserved sources from an available mixture observed by sensors. In other words, ICA makes it possible to separate independent data from a set of observable data. Many algorithms have been developed to perform ICA (*e.g.*, Maxkurt [Cardoso 1999], JADE [Cardoso 1999], Infomax [Touretzky et al. 1996], fastica [Bingham and Hyvarinen 2000; Cardoso 1998; Lee 1998]).

Independent component analysis finds a linear coordinate system (the unmixing system) such that the resulting signals are statistically independent. Derived from (1) and not taking noise into account (*i.e.*, $u(t) = 0$) is the ICA model

$$x(t) = A.s(t) \tag{A.5}$$

where A is an $M \times L$ scalar mixing matrix, in which M is the number of observations and L is the number of sources recovered. The goal of ICA is to find a linear transformation W of the observed matrix x that makes the output as independent as possible:

$$z(t) = W.x(t) = W.A.s(t) \tag{A.6}$$

where z is an estimate of the sources. The sources are recovered when W is the exact inverse of A up to a permutation, sign and scale change. These methods work well when the noise level is low (typically a signal-to-noise ratio $>$20 dB); their advantage is that they are the fastest techniques. However, because of the presence of high noise in our application, we used techniques including noise in the mixture model. To reduce ICA drawbacks in terms of noise, Attias (1999) proposed a model in which the source distributions are a mixture of Gaussians, the parameters of which are to be estimated jointly with the mixing matrix. Moreover, previous studies on ICA and blind source separation assume that the source distributions are sparse. Sparsity is the case where the data can be represented by a very small number of coefficients; that is, most of the source data coefficients are close to zero. Applying a transformation such as discrete cosine transform or wavelet transform to the original data can be considered sparse. Sparsity can improve ICA for two reasons: first, the statistical accuracy with which the mixing matrix can be estimated is related to how non-Gaussian the source distributions are; second, given A, the quality of the source estimates is also better for sparser sources.

Davis and Mitinoudis (2004) proposed a method that assumes the source distributions to be sparse using Mallat's modified discrete cosine transform (Mallat 1998). This technique referred to as sparse blind source separation uses two Gaussian vectors to model the distribution of source coefficients: one "on" state corresponding to a high-variance Gaussian vector, and one "off" state corresponding to a small variance. It estimates the mixing matrix, the noise covariance and the weights in the mixture of Gaussians with an expectation maximization–based procedure. Source recovery is performed using the least mean square method.

APPENDIX C

SUPPORT VECTOR MACHINE CLASSIFICATION

Given the training data set $S = \{\mathbf{x_i}, y_i\}$, with $\mathbf{x_i} \in \mathbf{R^d}$ the training vectors and $y_i = \{-1; +1\}$ the associated classes, we used the canonical form for SVM, which searches for the optimal hyperplane characterized by a normal $\mathbf{w}$ and an offset b that gives the maximum margin and satisfies the constraint

$$y_i(\mathbf{w}.\mathbf{x_i} + b) \geq 1 - \xi_i \quad i = 1, 2, \ldots \tag{A.7}$$

where the ξ_i are a set of positive slack variables, and "." is the inner product. Each vector may be at a distance $\xi_i / \|\mathbf{w}\|$ on the wrong side of the margin hyperplane. The ξ_i are a measure of the misclassification error, and the penalty function is then given by

$$C\sum_{i=1}^{n} \xi_i \tag{A.8}$$

where C is a parameter chosen by the user. A larger C corresponds to a higher penalty for errors. It is a convex optimization problem, the aim of which is to find the global minimum. Through reformulation of the problem using the Lagrangian multiplier method, the solution is given by the saddle point of the Lagrange function

$$L_p = \frac{1}{2}\|\mathbf{w}\|^2 + C\sum_{i=1}^{n} \xi_i - \sum_{i=1}^{n} \alpha_i(y_i(\mathbf{w}.\mathbf{x_i} + b) - 1 + \xi_i) - \sum_{i=1}^{n} \beta_i \xi_i \tag{A.9}$$

where the (α_i, β_i) terms are a set of non-negative Lagrangian multipliers. The minimum of the Lagrangian function is computed with respect to $\mathbf{w}$ and b. By setting the respective derivative and substituting these solutions, we obtain the dual objective function:

$$L_D = \frac{-1}{2}\sum_{i=1}^{n}\sum_{j=1}^{n}\alpha_i\alpha_j y_i y_j \mathbf{x_i}.\mathbf{x_j} + \sum_{i=1}^{n}\alpha_i \quad \text{(A.10)}$$

The minimum solution of the primal problem can be obtained by maximizing the dual objective function:

$$\tilde{\alpha} = argmax_\alpha\left(\frac{-1}{2}\sum_{i=1}^{n}\sum_{j=1}^{n}\alpha_i\alpha_j y_i y_j \mathbf{x_i}.\mathbf{x_j} + \sum_{i=1}^{n}\alpha_i\right) \quad \text{(A.11)}$$

$$\mathbf{s.t.} \quad C \geq \alpha_i \geq 0 \ \forall i \quad \text{and} \quad \sum_{i=1}^{n}\alpha_i y_i = 0 \quad \text{(A.12)}$$

The support vectors are the data points denoted $\mathbf{x_s}$for which $y_i(\mathbf{w}.\mathbf{x}+\mathbf{b})-1+\xi_\mathbf{i} = 0$ and $\alpha_i \neq 0$. They lie at a distance $\xi_i/\|\mathbf{w}\|$ on the wrong side of the margin hyperplane or on the margin hyperplanes denoted h_1, h_2 if $\xi_i = 0$. The optimal solution for the normal vector $\mathbf{w}$ is exclusively defined by the set of support vectors, and it can be written as a linear combination of these support vectors:

$$\tilde{\mathbf{w}} = \sum_{i=1}^{n}\tilde{\alpha}_i y_i \mathbf{x_i} \quad \text{(A.13)}$$

The optimal solution for the offset b can be obtained with

$$\tilde{b} = y_s - \sum_{i=1}^{n}\tilde{\alpha}_i y_i (\mathbf{x_i}.\mathbf{x_s}) \quad \text{(A.14)}$$

The optimal separating hyperplane is then given by

$$h(\mathbf{x}) = sign\left(\tilde{\mathbf{w}}.\mathbf{x}+\tilde{\mathbf{b}}\right) \quad \text{(A.15)}$$

where sign(.) is the sign function. The optimal linear boundary with the largest margin in the input space can be found using a restricted number of points called support vectors, which guarantee sufficient generalization power and robust behavior. In the case where a linear boundary in the input space is ineffective, the original space can be mapped into a high-dimensional space using a non-linear function, and the problem can be solved in this enlarged space. The mapping process is based on the chosen kernel K function satisfying Mercer's condition that

$$K\left(\mathbf{x_i}, \mathbf{x_j}\right) = \boldsymbol{\Phi}(\mathbf{x_i}).\boldsymbol{\Phi}\left(\mathbf{x_j}\right) \quad \text{(A.16)}$$

The input vectors appear only in the form of dot products in eqn (A.11), and by use of the kernel function in eqn (A.16), the optimization problem becomes

$$\tilde{\alpha} = argmax_\alpha\left(\frac{-1}{2}\sum_{i=1}^{n}\sum_{j=1}^{n}\alpha_i\alpha_j y_i y_j K\left(\mathbf{x_i}, \mathbf{x_j}\right) + \sum_{i=1}^{n}\alpha_i\right) \quad \text{(A.17)}$$

such that eqn (A.12) is true. The optimal separating hyperplane is then given by

$$h(\mathbf{x}) = sign\left(\sum_{i=1}^{n}\mathbf{y_i}\alpha_\mathbf{i}\mathbf{K}\left(\mathbf{x_i}, \mathbf{x_j}\right) + \mathbf{b}\right) \quad \text{(A.18)}$$

The more general case (where a linear boundary in the input space is inappropriate using a mapping function) can be solved. It can be shown that a SVM is able to exploit very high dimensional space with strong generalization guarantees derived from the max-margin property.